JOURNAL OF SPACECRAFT AND ROCKETS
Vol. 35, No. 6, November–December 1998

Mass Spectrometric Analysis of Reaction Products of Fast Oxygen Atoms-Material Interactions

Bertrand Cazaubon,* Alain Paillous,† and Jean Siffre‡
ONERA–CERT, 31055 Toulouse, France
and
Roger Thomas§
Laboratoire de Physique et Chimie de l'Environnement, 45071 Orléans, France

To study the reaction products of atomic oxygen impingement on spacecraft external materials, a quadrupole mass spectrometer coupled to transfer ion optics has been integrated into a space simulation chamber, equipped with a laser-assisted source of fast oxygen atoms. The mass spectrometer is used in a time-of-flight mode, which makes it possible to separate the effects of uv–vuv photons, oxygen ions, and oxygen atoms, all of which are present simultaneously in the pulsed neutral beam. Neutral surface reaction products are ionized either by charge transfer or by nonresonant laser multiphoton ionization. Initial studies on three polymer samples evidence a high analytical sensitivity, making it possible to detect and to differentiate the reaction products. Comparison between mass spectra data and direct mass loss measurements on several polymeric materials shows the semiquantitative aspect of the analysis technique that has been developed.

Introduction

OXYGEN atoms in low Earth orbit (LEO) at altitudes of between 200 and 900 km, combined with high orbital velocities, give rise to hyperthermal reactions on satellite surfaces. An average value of the O-atom number density at 400 km is on the order of 10^8 atoms $\cdot$ cm^{-3}. A spacecraft orbiting at 8 km/s impinges on a flux varying between 10^{13} and 10^{15} O-atoms $\cdot$ cm$^{-2} \cdot$ s^{-1}, depending on the altitude, solar activity, season, variation in the Earth's magnetic field, and latitude. The collision energy is approximately 5 eV. Spacecraft material surfaces are degraded by the hyperthermal oxygen atoms upon impact, as shown by postflight analysis of polymers and paint surfaces exposed during Space Shuttle flights, e.g., STS-5, STS-8, and STS-46.[1–5] Polymers suffer weight loss, change in various properties, loss of surface gloss, and premature aging. Erosion of surface materials by fast O-atoms is accompanied by emission of volatile reaction products. These constitute a possible source of contamination for critical parts of spacecraft on which they can condense. This contamination leads to a modification of the properties of thermal control coatings and thermal blankets, reduction of the electrical yield of the solar arrays, and degradation of the performance of optical components. It is therefore important to study this contamination problem and the material erosion mechanism caused by atomic oxygen (AO) in LEO.

A characterization method has been developed and adapted to Chambre Adaptée pour Simulation de l'Oxygène Atomique sur Revêtements (CASOAR), a space simulation chamber employing a laser-assisted source of fast oxygen atoms. A quadrupole mass spectrometer (QMS) has already been used to characterize the CASOAR's fast AO pulsed beam.[6] It was chosen here to analyze the species evolved by surfaces bombarded with fast O-atoms in the same facility. A flight experiment Evaluation of Oxygen Interactions with Materials III (EOIM III) has also employed a QMS technique for a similar purpose in the past.[7,8] Mass spectra of oxidation products obtained from organic polymers have been published; these products were studied without consideration of the energy and nature of the species present in the fast O-atom source.[9–13] In the present study, the earlier time-of-flight (TOF) characterization of all of the species present in the AO source and the QMS technique coupled with an ion transfer optics in a TOF measurement enabled us to separate the effects of ultraviolet–vacuum ultraviolet (uv–vuv) photons in synergy with oxygen ions and oxygen atoms, present in the AO source, which can improve our understanding of material degradation mechanisms. Here, ionization of the volatile neutral products has been realized either by charge transfer with the charged species present in the CASOAR O-atoms beam or by nonresonant multiphotonic laser ionization. After ionization, the products present in the vicinity of the sample surface have to be transmitted to the mass analyzer in the most efficient manner. An ion transfer optics has been developed. Application of the QMS to this study requires some adaptations that will be indicated here. Then we will describe the experimental setup (including the ion optics) and the data acquisition system. Finally, depending on the chosen analysis configuration, experimental results obtained with different polymeric materials will be presented.

Experiment

AO Source

The AO source used in CASOAR involves a pulsed laser-induced breakdown (PLIB) of molecular oxygen. This technique, described elsewhere,[14] delivers a pulsed beam at 8 km/s, with a typical fluence of 3×10^{15} atoms/cm^2 per shot at 40 cm from the source. The AO beam delivered by CASOAR contains fast neutrals and ions; results of mass spectrometry measurements[6] giving the beam composition are reported in Table 1. Ultraviolet (uv) and vacuum ultraviolet (vuv) photons with wavelengths as low as 60 nm were also produced during the initial oxygen plasma formation within the nozzle.

Mass Spectrometer

The Balzers QMA420 QMS, already used to characterize the CASOAR pulsed beam,[6] was employed to analyze the incoming reaction products from the reaction between this beam and materials. The reaction products appeared temporarily, for a few tens of microseconds, according to the time distribution of the O-atom pulses. The maximum velocity of the spectrometer mass scanning does not allow species with such a short time distribution to be analyzed. To solve this problem, product analysis must be carried out in sample mode; i.e., the mass spectrometer is set at the mass of the product that has to be detected. After ionization, the oxidation products are introduced in the QMS by means of collection and ion transfer optics. The total number of ions transmitted via the ion

Received June 23, 1997; revision received Feb. 23, 1998; accepted for publication Feb. 23, 1998.

*Research Engineer, Département Environnement Spatial, 2 av. Edouard Belin, BP 4025.
†Senior Research Engineer, Département Environnement Spatial, 2 av. Edouard Belin, BP 4025. Member AIAA.
‡Member of Technical Staff, Département Environnement Spatial, 2 av. Édouard Belin, BP 4025.
§Research Engineer, 3 av. de la Recherche Scientifique.

Table 1 Different species in the AO pulsed beam at 8-km · s^{-1} velocity

Species	Velocity, km · s^{-1}	Fluence per pulse, species · cm^{-2}	Relative quantity
O	8 ± 15%	2.9×10^{15}	91%
O_2	8 ± 15%	2.6×10^{14}	9%
O^+	10.6 ± 15%	7.9×10^{10}	25 ppm
O_2^+	10.9 ± 15%	1.4×10^{10}	5 ppm

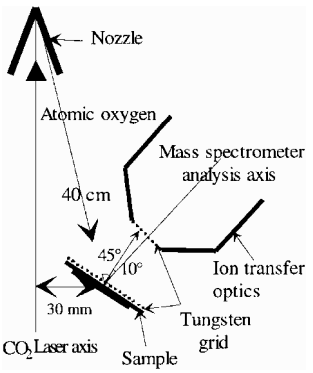

Fig. 1 Sample exposure to O-atom beam in CASOAR.

optics is large enough to obtain at the exit of the QMS secondary electron multiplier (SEM) an electron current that can be visualized directly on the load resistance of a digital oscilloscope. This technique allows one to record the time distribution of the ions hitting the SEM conversion dynode. The load resistance must be high enough to visualize signals of a few millivolts but as low as possible to minimize the time constant of the measuring line to avoid modification of the TOF distributions. Analysis is carried out mass by mass, in steps of 1 mass unit, from 0 to 200 amu. The signals obtained are digitized and stored in files for further integration. All of this makes the study longer than is usual when working in the mass scanning mode. Peak intensities in the histograms presented in this paper correspond to the integration of the analog signals visualized on the oscilloscope. The studied material sample was placed at 40 cm from the nozzle throat and on the propagation axis of the ions in the quadrupole; this axis formed a 50-deg angle with the propagation axis of the CO_2 laser used for the PLIB. The sample was located 3 cm from the CO_2 laser axis; the beam containing the O-atoms impinged on the sample at its center, with a 45-deg angle to the normal (Fig. 1). The entrance of the collection ion optics was 12 mm from the sample surface; this distance was minimized to obtain a wide collection opening. The distance between the ion optics entrance and the QMS was 190 mm. High vacuum pumping of the spectrometer head was performed to raise the signal/noise ratio, using a 400-l/s turbomolecular pump. The neutral oxidation products that were desorbed from the sample surface in the absence of charged species in the O-atom beam were ionized by a uv laser beam delivering 266-nm photons, corresponding to the fourth harmonic of a Quantel YAG laser. This laser beam, 10 mm in diameter, was introduced into the CASOAR vacuum chamber from the top, via three mirrors and a silica window (Fig. 2). It was tangent to the sample surface; care was taken to avoid laser ablation of the surface by the beam.

Optics for Collection and Transfer of Ions

The cations, created near the sample surface, were introduced into the ion optics by means of an extracting electron field. This field was obtained with a tungsten grid (150-μm mesh, giving 80% transparency) placed in close contact with the sample surface and biased to a positive potential and a second similar grid, located 10 mm from the sample at the ion optics entrance, at ground potential. A software program (SIMION, developed by the Idaho National Engineering Laboratory[15]) allowing ion trajectories in electric and magnetic fields to be computed was used to design the ion optics. Knowing the sample position relative to the ion optics entrance, we simulated the trajectories from three positions on the sample surface for 44 amu ions. For each position, ions were emitted within one half-space in 15-deg steps, assuming 1-eV kinetic energy desorption (Fig. 3).

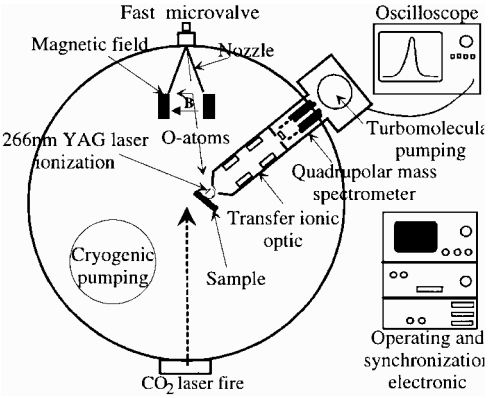

Fig. 2 Experiment with nonresonant multiphoton YAG laser ionization.

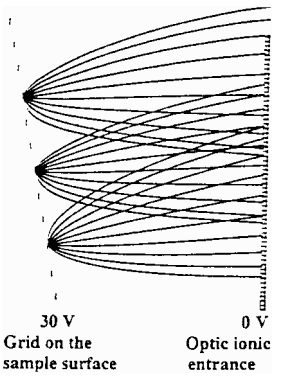

Fig. 3 Trajectory simulation of CO_2^+ ions, having 1-eV initial kinetic energy from three points on the sample surface.

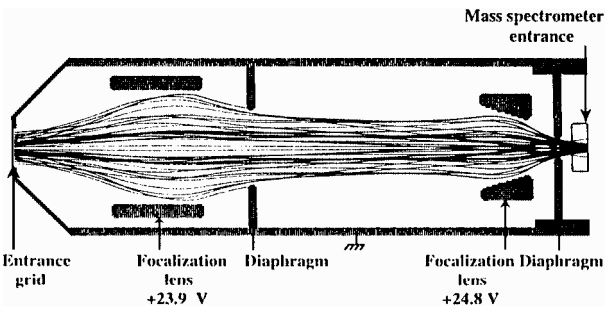

Fig. 4 Trajectory simulation of 31-eV CO_2^+ within the transfer ion optics.

This energy corresponds to the maximum kinetic energy at which oxidation products can be evolved upon 5-eV O-atom impingement. The potential difference must not exceed 50 V to avoid giving ions a kinetic energy that is too high for good filtering in the quadrupole; the simulation shows that a 30-V potential difference between the two grids is sufficient to collect a large part of the cations. The optics dimensions were determined by geometry constraints; 190 mm in length and entrance diameter equal to 20 mm. The optics aims at good transmission of the collected ions and optimum introduction into the quadrupole for filtering, i.e., concentration in the center of the QMS entrance (2.5-mm diam) and trajectories parallel to the axis. After many trajectory simulations, using the entrance conditions through the grid (positions, velocity, and angles) defined earlier, the following optical system was selected: a first ion lens, biased to 24-V potential, and a grounded diaphragm are used to collimate the ions; a second ion lens, biased to about 25 V, and a grounded diaphragm are used to concentrate the ions at the entrance of the mass spectrometer.

Figure 4 shows trajectories of CO_2^+ ions ($m/q = 44$), desorbed from a sample with a kinetic energy of 1 eV. This simulation result indicates that a great majority of the ions emitted into the complete half-space will be introduced in the mass spectrometer in optimum conditions to ensure mass filtering by the quadrupole.

Nonresonant Laser Multiphoton Ionization

Nonresonant multiphoton laser ionization with photons at 266-nm wavelength, i.e., 4.66-eV energy per photon, makes it possible to ionize almost all organic compounds, which have potential ionization between 6 and 12 eV, by absorption of $2 + 1$ photons. The main interest of this technique is that the exact nature of the incoming products from the interaction of fast O-atoms and polymer materials does not need to be known beforehand. In the present study, most of the reaction products are unknown. However, they are all organic compounds, and therefore they can be ionized by the nonresonant multiphotonic laser technique. Compared with other uv sources such as deuterium lamps, a YAG laser has evident advantages because of its high photon density and directionality, increasing the ionization probabilities. Here, by using a laser beam ionization, it is also possible to limit the disturbances caused by background products because only the charged species present in the volume resulting from the intersection of the laser beam and the locus of the electric field created by the tungsten grids will be introduced in the mass spectrometer. For a YAG laser delivering 90-mJ laser pulses of 10-ns width, the power density within a 10-mm beam is 12 $MW \cdot cm^{-2}$, which is sufficient to ionize a large amount of molecules.[16,17] One major problem in using the nonresonant multiphotonic laser ionization technique is the perfect synchronization between the YAG laser firing and the fast O-atoms pulse reaching the sample surface. This was solved by means of synchronization electronics and a pulse generator, making it possible to adjust the laser firing with the O-atom beam on the sample surface, at a pulse repetition rate of 2.4 Hz, with an accuracy of 1 μs.

Material Test Procedure

The sample (1 cm^2) studied under the CASOAR pulsed beam was inserted between a metallic plate and a tungsten grid (150-μm mesh, allowing 80% transmission) that were biased at the same positive voltage. The ionized products emanating from the sample were introduced into the quadrupole mass filter, via the ion optics, by means of the extraction electric field. At the quadrupole exit, the filtered ions were directed to the SEM to be converted and amplified into an electronic current; signals were visualized on an oscilloscope using a 120-kΩ load resistance. Once these signals obtained with successive AO pulses had been averaged over eight shots, they were digitized and stored in a file to be processed in a data processor. Product analysis was carried out in two steps. First, a fast mass scanning from 0–200 amu was performed, applying to the ion optics the standard voltage found during the trajectory simulation study with SIMION. The ion source parameters were chosen to give a mass separating power Δm less than one unit. Then the mass spectrometer was put in a sample mode on the heavier ion mass found previously, and the potential values were optimized to obtain the most intense signal on the oscilloscope; the mass resolution was also optimized to ensure that the signal value was zero between two products separated by one mass unit. Parameters thus obtained were kept constant for all masses to permit relative quantitative analysis of the different products, assuming that transmission and filtering remained the same in the mass range 0–200 amu. Mass spectra of oxidation products were determined, under bombardment by the CASOAR beam, in two test configurations: 1) with the raw beam, composed of all fast neutral and charged species, plus the uv–vuv photons emitted by the source (in this configuration the reaction products were ionized by charge transfer with the charged species present in the O-atom beam) and 2) with a neutral beam, cleared out by removal of its charged species by means of a magnetic field placed at the exit of the nozzle (in this configuration the reaction products cannot be ionized by charge transfer, and so they must be ionized before QMS measurement, using nonresonant multiphoton laser absorption at 266-nm wavelength).

Background Products of the Measuring Line

In practical experimental conditions, several parasitic products may be added to the reaction products: oxidation products resulting from interaction of the large O-atom beam with all materials present in the chamber, background gas, contamination (especially on the sample tungsten grids), and molecular oxygen obtained by recombination of oxygen on the surface. In our experiments, a tungsten grid was always employed on the sample surface. Therefore, a subtraction of these parasitic products had to be performed; this was carried out by subtracting the products spectrum obtained with a tungsten plate for the complete mass range from 0 to 200 amu, in 0.2-amu mass steps (Fig. 5) from the sample spectra. Between 0 and 16 amu products are not shown because filtering by the quadrupole was disturbed by the excessive quantities of hydrogen and AO that were present in the chamber. It was not possible to solve this problem by raising the mass resolution to a maximum because this considerably reduced the sensitivity for heavy mass products. Therefore, information related to species with a mass lower than 16 amu is not available in the mass spectra presented next.

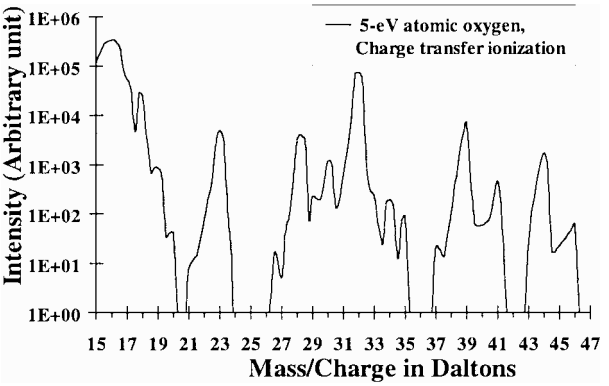

Fig. 5 Background noise measured on the empty sample holder, under action of the CASOAR raw beam.

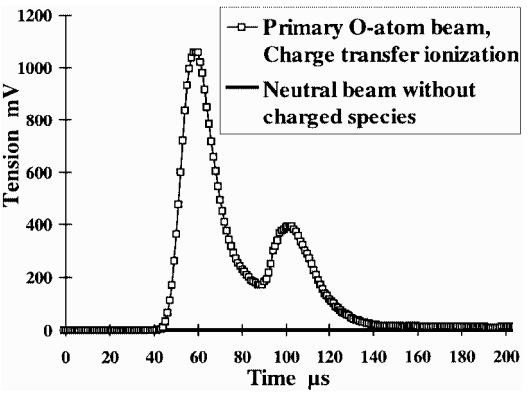

Fig. 6 Analog signal at m/q = 44 obtained on FEP with the raw beam and with the CASOAR neutral beam.

Analog Signal Relative to Reaction Products Obtained by Interaction of the CASOAR Raw Beam with Materials

Figure 6 shows the general shape of the signals obtained for oxidation products; this figure is related to species ionized by charge transfer, at the mass/charge ratio $m/q = 44$ (CO_2^+). The signal displays two peaks at 60 and 100 μs. The origin of the time axis corresponds to the CO_2 laser firing, creating the AO beam in the nozzle. The time appearance of these peaks can be decomposed into two parts: 1) TOF of the beam species from the nozzle to the sample, located 40 cm from the nozzle throat and 2) TOF of the reaction products from the sample surface to the SEM, through the transfer ion optics and the mass filter.

Because the ionized products have the same kinetic energy on exiting from the extracting electric field, their TOF to the SEM is the same. Therefore, the two distinct peaks are due to a difference in the TOF of the CASOAR beam components responsible for the creation of those products. The first peak is due to the fastest species contained in the beam, i.e., the O^+ and O_2^+ ions. A previous study[6] indicates that these primary ions travel at 11 km/s, with a TOF of about 35 μs from the nozzle to the sample; the TOF between sample and SEM for ionized oxidation products that is computed, at $m/q = 44$ under an extracting electric field of 40 V, is about 25 μs; this corresponds to a total TOF of approximately 60 μs. The

second peak is due to the neutral species, O and O_2. The TOF of this neutral species from the nozzle to the sample is about 50 μs at 8 km/s. The TOF of the formed species at 44 amu is always 25 μs, giving a total TOF of approximately 75 μs. However, Fig. 6 shows that the second peak is delayed by about 20 μs when compared with this theoretical TOF. Such a delay could be due either to an ionization of the oxidation products occurring at a greater distance from the sample surface or to a time delay caused by the potential barriers of the electrodes in the ion optics. The charged species in the CASOAR raw beam can be efficiently suppressed using a magnetic field placed transversally to the beam expansion at the nozzle exit (see the next section). Figure 6 shows that the mass signal disappears when the charged species are no longer present in the O-atom beam; therefore, the ionization of the reaction products can be attributed to a charge transfer between these neutrals and the ions present in the CASOAR beam. The charge transfer is possible as a consequence of an overlapping of the time distributions of ions and neutrals in the raw beam. The absence of a signal with the AO beam without the charged species indicates that the formed products are predominantly neutral. The TOF difference between ions and neutrals in the O-atom beam gives us the species responsible for the formation of products. By separately integrating the two peaks, distinct mass spectra due to the action of oxygen ions and oxygen atoms can be obtained.

Analog Signal Relative to Products Obtained by Interaction Between the AO Beam and Materials

Ferrite permanent magnets, delivering a 0.14-T magnetic field, make it possible to deflect with 4.7-cm curve radius O_2^+ ions with a velocity of 20 km $\cdot$ s^{-1}. This has been verified experimentally by means of a Langmuir probe,[18] and the technique has been employed for delivery of a neutral beam in the CASOAR. The neutral reaction products were ionized by nonresonant multiphotonic laser absorption at 266 nm. Figure 7 shows an analog signal obtained, at $m/q = 44$, on a fluorinated ethylene-propylene (FEP) sample bombarded with such a neutralized beam of O-atoms. The first peak, a, with an intensity of approximately 5 mV, corresponds to the electromagnetic noise produced by CO_2 laser firing. Peak b, about 2 mV, corresponds to a photoelectron emission on the SEM converting dynode; it was induced by the uv–vuv photons emitted during initial oxygen plasma formation within the nozzle. Although the mass spectrometer was not in the uv–vuv propagation axis, photons entered the mass spectrometer after reflecting off the chamber's metallic walls; a similar observation was made when the EOIM-III QMS was under ground calibration.[19] Peak c, located at 60 μs, corresponds to the action on FEP of a few oxygen ions that were not deviated by the magnetic field. Lastly, peak d, at 100 μs, corresponds to reaction products resulting from interaction of the AO beam with FEP, which were ionized by nonresonant multiphotonic absorption. The time delay on the delay generator was adjusted to synchronize exactly the YAG laser pulse and the arrival of AO on the sample surface, i.e., 50 μs after firing the CO_2 laser. The broad time distribution of the products ionized by the YAG laser pulse, which is only 10 ns in duration, is due to the fact that the reaction

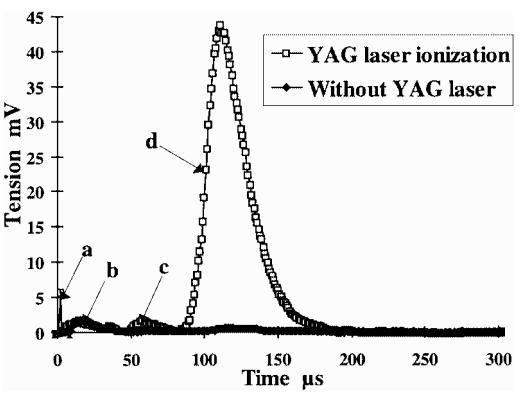

Fig. 7 Analog signal at m/q = 44 measured on FEP under action of the neutral beam.

Table 2 Experimental conditions for AO source, mass spectrometer, and YAG laser

Parameter	Value
Fire frequency, Hz	2.4
Time delay between microvalve opening and CO_2 TEA laser firing, μs	475
Molecular oxygen flow, cm^3/mn	10
CO_2 TEA laser energy per pulse, J	10 ± 5%
Sample grid polarization, V	44
SEM polarization, V	2400
YAG laser energy at 266 nm, mJ/pulse	90
Power density, MW/cm^2	12
YAG laser delay after O-atom formation, μs	50

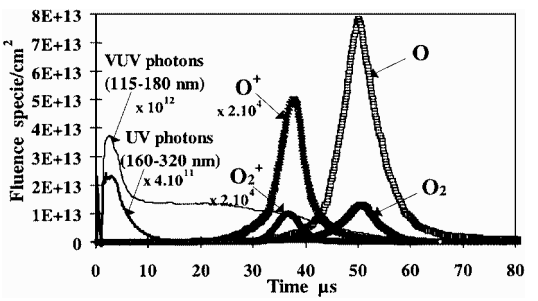

Fig. 8 Time distribution of species in the raw beam at the sample location.

products, which are ionized by the laser beam (10 mm in diameter), are not extracted by the same electric field, thus giving different TOF in the apparatus. This large distribution could also be due to different ion trajectories in the ion transfer optics. Comparison of the signal obtained by laser ionization with that obtained by charge transfer confirms that the second peak obtained under the O-atom raw beam corresponds to the action of AO because it appears at the same time as the one obtained with laser ionization. A small time delay observed between the two peaks relative to the O-atom action confirms the charge transfer ionization of neutral products with charged species of the beam: because the time distribution of ions and neutrals in the beam have only overlapped partially (Fig. 8), only products from the fastest O-atoms can be ionized.

Test Results on Polymer Samples

Experimental Conditions

Testing with 8-km $\cdot$ s^{-1} O-atoms was carried out on fluorinated polymers, in the two configurations indicated earlier. Table 2 gives the AO source and YAG laser parameters, when the charged species are removed from the O-atom beam and product ionization is obtained by multiphoton absorption at 266 nm. QMS resolution is insufficient to determine exactly the chemical composition of the detected ions. Therefore, in the following mass spectra, only a tentative assignment of the peaks to a chemical composition of ions is given. The composition of reaction products was estimated by associating the atomic species present in the material's chemical formula and oxygen atoms.

FEP

Transparent FEP films are used as flexible solar reflectors, thermal insulation multilayers, and substrates for special usages. The chemical structure is

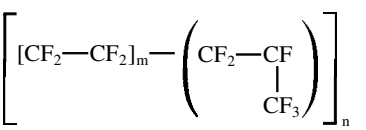

Figure 9 shows the mass spectrum of products obtained during interaction of FEP with the AO beam containing oxygen ions. The relative intensity, at each mass, results from a peak integration of the analog signal, appearing at about 60 μs and recorded on the oscilloscope (see Fig. 6), after subtraction of the blank signal measured on

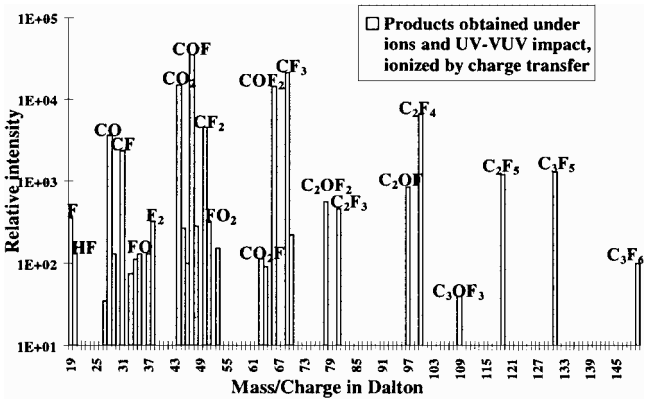

Fig. 9 Mass spectrum of the products resulting from interaction between FEP and the ionic part of the CASOAR raw beam (ionization by charge transfer).

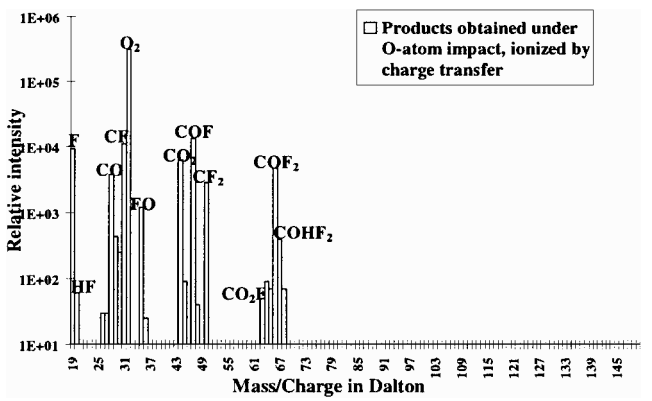

Fig. 10 Mass spectrum of the products resulting from interaction between FEP and the neutral part of the CASOAR raw beam (ionization by charge transfer).

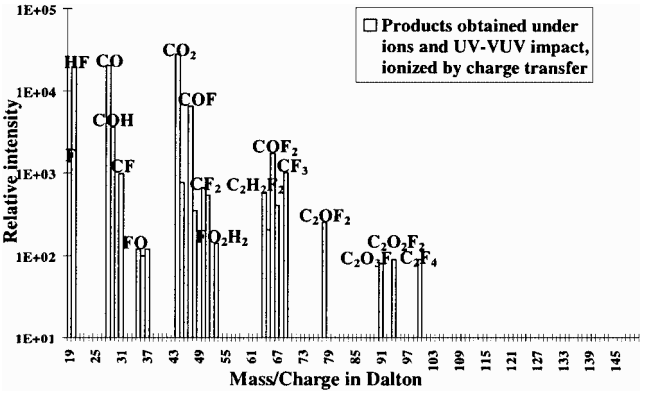

Fig. 11 Mass spectrum of the products resulting from interaction between PVDF and the ionic part of the CASOAR raw beam (ionization by charge transfer).

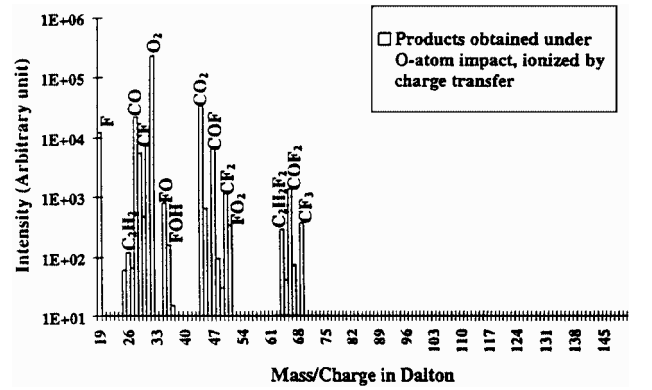

Fig. 12 Mass spectrum of the products resulting from interaction between PVDF and the neutral part of the CASOAR raw beam (ionization by charge transfer).

the empty sample holder covered with the same grid as used to material measurements. The mass range was scanned from 0 to 200 amu, in 1-amu steps. The mass spectrum, showing mainly oxygenated products with light mass, indicates a predominant process of chemical damage by oxidation. However, the presence of nonoxygenated fluorocarboned products, in nonnegligible quantity and corresponding to polymer chain fragments such as CF^+, CF_2^+, CF_3^+, $C_2F_4^+$, and $C_3F_6^+$, suggests a damage process by collision bond breaking by the ions and/or depolymerization by vuv photons. In this spectrum, all of the products obtained by Cross and Koontz[9] with FEP under O-atoms and vuv bombardment are present, along with heavier products such as $C_3F_6^+$. Similarly, Fig. 10 shows the mass spectrum of products obtained under only O-atom impact. The products formed are only oxygenated products; the nonoxygenated fluorinated products have disappeared. O-atoms with 5-eV kinetic energy do not have sufficient energy to break C—C bonds. Catherine[20] indicates that the energy required to create erosion by a collision process is approximately three times the bond energy. The C—C bond energy is 3.6 eV (Ref. 21); consequently, bond breaking of the monomer seems easier with O^+ and O_2^+, with respective energies of about 10 and 20 eV, than with the O-atoms of CASOAR, which have a kinetic energy of about 5 eV. It is important to note that the fluorinated fragments could also be produced by vuv photons, created during plasma formation in the nozzle, with complementary ionization by charge transfer with ions. This mechanism is possible because of a time overlap of the distribution of vuv photons (emitted in the 115–180 nm wavelength range) with that of beam ions on the sample surface (Fig. 8). Emission of high mass fluorocarboned products, such as C_mF_n, by FEP under vuv photons has already been shown.[9,22,23] According to results reported by Koontz et al.,[24] FEP appears to have a weak reactivity to AO in the absence of vuv photons. This is confirmed by the mass spectrum in Fig. 10. The production of fluorocarboned compounds under vuv radiation is undeniable; however, in Fig. 9, the fluorocarbon products could also be the result of a collision process with oxygen ions. The use of an optical chopper, stopping the uv–vuv photons while maintaining the O-atoms, would have made it possible to determine more exactly the origin of the degradation products, but this would be a difficult and expensive task and has not been carried out in the present study.

Polyvinylidene fluoride (PVDF)

PVDF films are used on account of their piezoelectric properties. The chemical structure is $[CH_2—CF_2]_n$.

Figures 11 and 12 show mass spectra of the products, respectively, obtained under the action of the ions and oxygen atoms of the raw beam; in both cases these products were ionized by charge transfer. The spectra are similar to those obtained with FEP. Most of the products were oxygenated carboned compounds, but there are also some hydrogenated products. Fluorocarboned products were not observed at masses higher than 100 amu. Products similar to CH_2CF_2 fragments in which hydrogen atoms have been substituted by oxygen atoms appeared at high masses such as 78, 91, and 94 amu. However, these products were in small quantities compared with products such as HF, CO, CO_2, or COF. Figure 13 shows the mass spectrum of products obtained with a neutral oxygen beam and that have been ionized by nonresonant laser multiphotonic absorption; the products are logically the same as those in Fig. 12; nevertheless the hydrogenated products were larger. This may be attributed to an easier ionization of hydrogenated compounds, which are less electronegative than the oxygenated products.

Polyethersulfone (PES)

A transparent PES film, 50 μm thick, was studied. PES can be used as structural polymer or as matrix in composite materials on spacecraft. Its chemical structure is $[C_6H_4—SO_2—C_6H_4—O]_n$.

Identification of the peaks corresponding to sulfured products was facilitated by the presence of the S^{34} isotope, corresponding to about 4% of S^{32}. The mass spectra (Figs. 14 and 15) were obtained with the

Table 3 Evaluation of AO reactivity measured in CASOAR and correlation between mass loss estimated from QMS and directly measured

Sample	Reactivity, cm^3/atom			Ratio of mass loss with and without ions in the CASOAR beam	
	CASOAR with ions	CASOAR without ions	LEO[8,25]	Calculation from mass spectra	Measurement by weighing
FEP	1.9×10^{-24}	0.4×10^{-24}	$0–0.05 \times 10^{-24}$	4.5	4.1
PTFE	1.2×10^{-24}	0.5×10^{-24}	$0–0.06 \times 10^{-24}$	2.3	2
PVDF	3×10^{-24}	1.6×10^{-24}	0.6×10^{-24}	1.9	1.7
PVDC[a]	4.6×10^{-24}	3.4×10^{-24}	——	1.4	1.4
E-CTFE[b]	2.7×10^{-24}	2.4×10^{-24}	0.9×10^{-24}	1.1	1.3
PPS[c]	1.9×10^{-24}	1.6×10^{-24}	——	1.2	1.2
PES	2.4×10^{-24}	2.1×10^{-24}	2.4×10^{-24}	1.2	1.05

[a]PVDC, polyvinyldichloride. [b]E-CTFE, polyethylene-chlorotrifluorethylene. [c]PPS, phenylenesulfide.

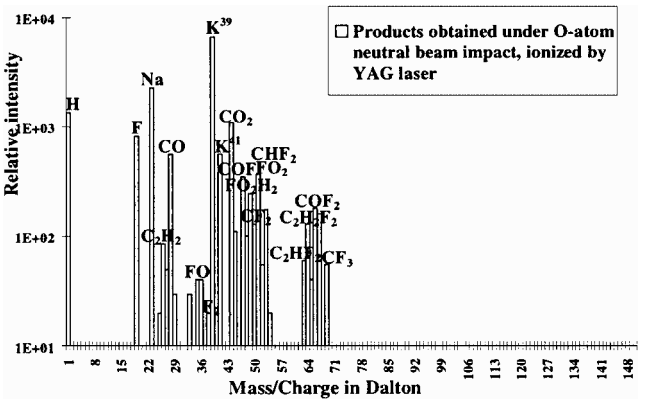

Fig. 13 Mass spectrum of the products resulting from interaction between PVDF and the neutral part of the CASOAR neutral beam (ionization by multiphotonic absorption).

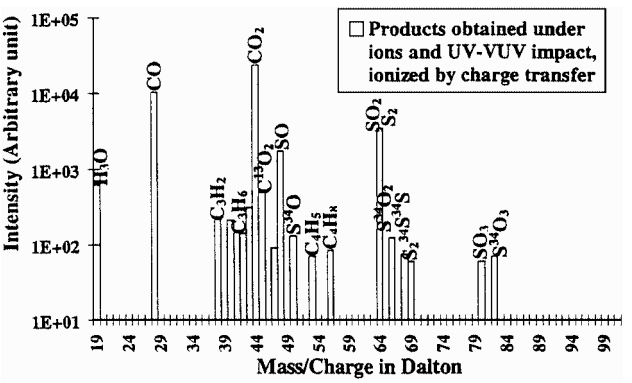

Fig. 14 Mass spectrum of the products resulting from interaction between PES and the ionic part of the CASOAR raw beam (ionization by charged transfer).

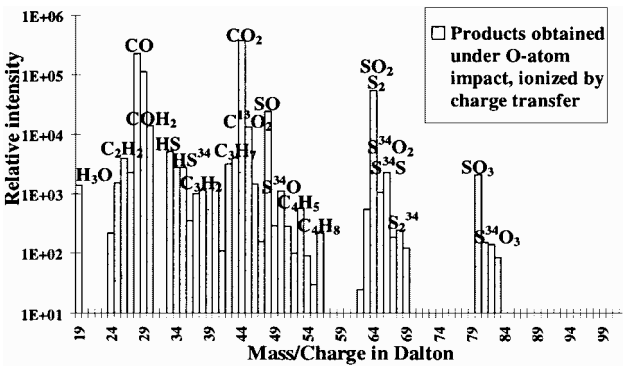

Fig. 15 Mass spectrum of the products resulting from interaction between PES and the neutral part of the CASOAR raw beam (ionization by charge transfer).

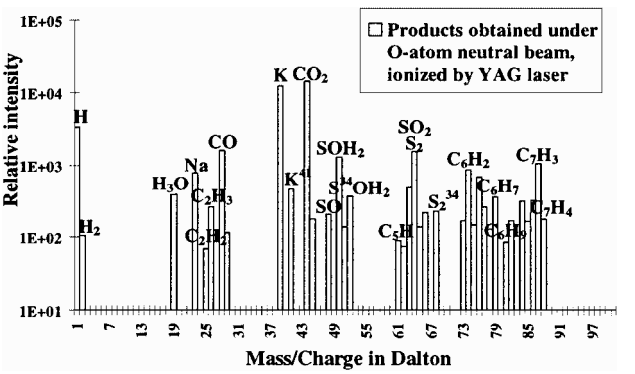

Fig. 16 Products mass spectrum obtained with PES under O-atom neutral beam.

O-atom raw beam. The emitted products, e.g., CO, CO_2, SO, SO_2, and SO_3, are typical of the photooxidation of sulfured polymers. The limited QMS resolution does not allow one to ascertain if the product at $m/q = 64$ was S_2 or SO_2: the presence of isotope S^{34} does not make it possible to obtain sufficient information here; however, SO_2 seems more probable because this product results from the action of the AO. Nonoxygenated hydrogenated carboned products incoming from the phenyl group were observed. In Fig. 16, the mass spectrum, obtained under a neutral AO beam, shows the same products as obtained with the raw beam (Fig. 15). Products corresponding to the phenyl group appeared; SO_3 was not observed.

Correlation Between Mass Spectrometry Measurements and Erosion Measurements

Oxygen ions that are present in the O-atom raw beam can have an influence on material degradation. This has been further evaluated. Mass loss measurements were performed on different materials bombarded with the CASOAR pulsed beam, at 8 km/s, with and without charged species present in this beam. The material samples were located 35 cm from the nozzle, in the central part of the beam. The samples were subjected to 50,000 beam pulses. Erosion data on several Kapton® polyimide reference samples, either surrounding the tested materials or replacing them, were also obtained while maintaining identical bombardment conditions. As compared with the mass loss found using the raw beam, i.e., neutrals plus ions, the Kapton mass loss was measured to be lower by 24% when this material was bombarded by AO without the charged species, keeping the same source parameters and an identical pulse number. A widely accepted value of Kapton reactivity is 3×10^{-24} cm^3/atom; this value was deduced from several flight experiments in LEO[25]; it is used to evaluate the O-atom fluences during ground simulation testing in most AO facilities all over the world, including in past experiments using the CASOAR raw beam. Application of the CASOAR erosion data would lead to different reactivities for Kapton, depending on the presence or absence of charged species. Using 3×10^{-24} cm^3/atom as Kapton reactivity under the CASOAR raw beam (neutrals + ions), the reactivity of the same material would be estimated to be only 2.3×10^{-24} cm^3/atom upon testing involving elimination of

the charged species. Similarly, Table 3 shows the reactivity coefficients derived from testing in CASOAR for some other polymers; it confirms that the effect of the charged particles on material degradation is serious, although they represent only a few parts per million compared with the quantity of O-atom in the beam. Fluorinated polymers seem to be particularly susceptible to ions, with a reactivity two times higher for polytetrafluorethylene (PTFE) and PVDF. For FEP the reactivity with ions is four times higher than measured without charged species. This great sensitivity of FEP toward ions can be put in parallel with data from Vered et al.,[26] who measured a reactivity of 6×10^{-22} cm^3/atom for FEP under irradiation with 30-eV oxygen ions. Chlorinated polymers present a reactivity that is 30% higher with ions. Sulfured polymers seem to be less sensitive to ions, with a reactivity about 15% higher to that obtained without ions. These reactivity coefficients have to be compared with those obtained on flight experiments in LEO and during tests in simulators with a similar AO source (Table 3). Reactivity coefficients found in CASOAR for halogenated polymers, with or without ions, are higher than those measured in LEO. This may be attributed to the uv–vuv photons produced during oxygen plasma formation in the nozzle, to which halogenated polymers are very sensitive. AO reactivity measured in simulators at the Los Alamos National Laboratory, Physical Sciences, Inc., or the European Space Research and Technology Centre, with an AO source similar to that used in CASOAR, is of the same order.[24,27,28] For PES, the reactivity coefficient is the same as that found in LEO. This shows that sulfured polymers are not sensitive to uv–vuv photons.

Using the mass spectra previously obtained, we tried to estimate the mass loss ratios obtained with and without charged species in the O-atom beam. For that purpose, the intensity of each mass peak was multiplied by the mass corresponding to this peak. Each mass was also corrected by subtraction of the amount of oxygen, considering the chemical composition attributed to the peak. A total mass loss was calculated by summing all of the weighed values of the peaks forming the mass spectrum. Table 3 gives the ratios obtained by dividing the total mass loss under the CASOAR raw beam (ions and AO) by the total mass loss under the CASOAR beam after elimination of ions. Table 3 also gives the ratios obtained from direct weighing of the sample mass loss using a microbalance. The fact that the same mass loss ratios were found, by weighing and by computation from the mass spectra, allows us to say that the QMS analysis of the incoming products from the interaction between AO and materials is also semiquantitative: the product quantities obtained for one material under ions and AO impact can be compared.

Conclusion

QMS, coupled with ion transfer optics, has enabled us to develop an analysis technique for incoming reaction products from the interaction between AO and materials. Probative tests have shown that this technique has great potential. It is easier and more informative than laser-induced fluorescence for detecting and identifying the reaction products. It has a high analytical sensitivity, and the products can be differentiated in most cases owing to a separating power of less than one unit. One disadvantage is that the method is time consuming (spectrum acquisition mass by mass, in one-mass unit steps; decomposition of TOF signal). Also, the detected products are ionic fragments rather than complete molecules, which leaves a great part to interpretation for the exact identification of species.

The mass spectra data obtained on several polymeric materials have shown that some reaction products, formed by interaction between AO and materials used on board, can be dangerous for spacecraft in LEO: contamination by condensation on cold surfaces of high molecular weight species and possible corrosion by acid species (such as SO_2 and SO_3). This information is important for assessing possible problems during missions.

Moreover, in addition to the initial use, which had been anticipated, this technique has thrown light on some aspects of damage mechanisms and more particularly on the respective action of ions, atoms, and uv–vuv photons. On one hand, this has allowed us to obtain a complete appraisal of the AO testing conditions in CASOAR and, on the other hand, to highlight the major degradation factors in a space environment (for example, the predominant action of vuv photons over AO for fluorinated polymers). Although not generally accepted as a TOF measurement method, quadrupole mass spectrometry in this particular configuration makes is possible to distinguish between the action of AO and that of oxygen ions reacting in synergy with uv–vuv photons, owing to their TOF difference in the simulation chamber. A comparative quantitative analysis of mass spectra obtained under the impact of ions and AO makes it possible to study the influence of oxygen ions on material. A comparative study with mass loss measurements has allowed us to show that the influence of ions on material degradation must be considered, even if they are in small quantity compared with oxygen atoms.

An efficient chemical product ionization phenomenon, by charge transfer with the charged species of the simulation beam, has also been evidenced. The ion flux, collected by samples 40 cm from the nozzle in our O-atom beam, is of a magnitude similar to that collected in LEO at 300-km altitude. Therefore the same ionization mechanism of neutral products by charge transfer may be expected in LEO conditions. This confirms that transport mechanisms involving charged species can definitely play a role in spacecraft contamination in these orbits. In conclusion, an interesting tool for improving our knowledge of the behavior of space materials behavior has been implemented. It could also be used in connection with other degradation sources such as electron beam and uv–vuv photon sources.

References

[1]Leger, L. J., Santos-Mason, B., Visentine, J. T., and Kuminecz, J. F., "Review of LEO Flight Experiments," *Proceedings of the NASA Workshop of Atomic Oxygen Effects*, Pub. 87-14, Jet Propulsion Lab., California Inst. of Technology, Pasadena, CA, 1987, pp. 1–10.

[2]Visentine, J. T., Leger, L. J., Kuminecz, J. F., and Spiker, I. K., "STS-8 Atomic Oxygen Experiment," AIAA Paper 85-0415, Jan. 1985.

[3]Zimcik, D., and Maag, C. R., "Results of Apparent Atomic Oxygen Reactions with Spacecraft Materials During Shuttle Flight STS-41G," *Journal of Spacecraft and Rockets*, Vol. 25, No. 2, 1988, pp. 162–168.

[4]Tennyson, R. C., Mabson, G. E., Morison, W. D., and Kleiman, J., "Preliminary Results from the LDEF/UTIAS Composite Materials Experiment," *Proceedings of the First LDEF Post-Retrieval Symposium*, NASA Conf. Publication 3134, Kissimmee, FL, 1991, pp. 1057–1072.

[5]Strganac, T. W., Letton, A., Rock, N. I., Williams, K. D., and Farrow, D. A., "Characterization of Polymer Films Retrieved from NASA's LDEF," *Journal of Spacecraft and Rockets*, Vol. 32, No. 3, 1995, pp. 502–506.

[6]Cazaubon, B., Paillous, A., Siffre, J., and Thomas, R., "Five-Electron-Volt Atomic Oxygen Pulsed-Beam Characterization by Quadrupolar Mass Spectrometry," *Journal of Spacecraft and Rockets*, Vol. 33, No. 6, 1996, pp. 870–876.

[7]Koontz, S. L., Leger, L. J., Rickman, S. L., Hakes, C. L., Bui, D. T., Hunton, D. E., and Cross, J. B., "Oxygen Interactions with Materials III—Mission and Induced Environments," *Journal of Spacecraft and Rockets*, Vol. 32, No. 3, 1995, pp. 475–482.

[8]Koontz, S. L., Leger, L. J., Visentine, J. T., Hunton, D. E., Cross, J. B., and Hakes, C. L., "EOIM-III Mass Spectrometry and Polymer Chemistry: STS 46, July–August 1992," *Journal of Spacecraft and Rockets*, Vol. 32, No. 3, 1995, pp. 483–495.

[9]Cross, J. B., and Koontz, S. L., "Ground-Based Simulation of LEO Environment: Investigation of a Select LDEF Material-FEP Teflon™," *Proceedings of a NASA Conference on LDEF Materials Results for Spacecraft Applications*, Publication 3257, NASA, Huntsville, AL, 1992, pp. 379–389.

[10]Cross, J. B., "Laboratory Investigations: Low Earth Orbit Environment Chemistry with Spacecraft Surfaces," Space Operations Automation and Robotics Workshop, LA-UR-89-2168, Houston, TX, July 1989.

[11]Cross, J. B., Spangler, L. H., Hoffbauer, M. A., Archuleta, F. A., Leger, L. J., and Visentine, J. T., "High Intensity 5eV AO Source and Low Earth Orbit Simulation Facility," *Proceedings of the NASA Workshop on Atomic Oxygen Effects*, Pub. 87-14, Jet Propulsion Lab., California Inst. of Technology, Pasadena, CA, 1987, pp. 105–117.

[12]Sonoda, K., Nishikawa, T., and Nakanishi, K., "Atomic Oxygen Effect on Physical Properties of Spacecraft Materials in LEO," AIAA Paper 89-1761, June 1989.

[13]Cross, J. B., Koontz, S. L., Gregory, J. C., and Edgell, M. J., "Hyperthermal Atomic Oxygen Reactions with Kapton and Polyethylene," *Proceedings of a Symposium at the 119th Annual Meeting of the Minerals, Metals and Materials Society* (Anaheim, CA), *Materials Degradation in Low Earth Orbit*, Minerals, Metals and Materials Society, Warrendale, PA, 1990, pp. 1–14.

[14]Caledonia, G. E., Krech, R. H., and Green, B. D., "A High Flux Source of Energetic Oxygen Atoms for Material Degradation Studies," *AIAA Journal*, Vol. 25, No. 1, 1987, pp. 59–63.

[15]Dahl, D. A., and Delmore, J. E., "The SIMIONS PC/PS2 User's Manual Version 4.0," Idaho National Engineering Lab., EG & G Idaho Inc., Idaho Falls, ID, April 1988, pp. 1–88.

[16]Goeringer, D. E., Glish, G. L., and McLuckey, S. A., "Fixed-Wavelength Laser Ionization/Tandem Mass Spectrometry for Mixture Analysis in the Quadrupole Ion Trap," *Analytical Chemistry*, No. 63, No. 13, 1991, pp. 1186–1192.

[17]Engelke, F., Hahn, J. H., Henke, W., and Zare, R. N., "Determination of Phenylthiohydantoin-Amino Acids by Two-Step Laser Desorption/Multiphoton Ionization," *Analytical Chemistry*, Vol. 59, No. 6, 1987, pp. 909–912.

[18]Cazaubon, B., "Etude par Spectrométrie de Masse Quadripolaire d'un Jet Pulsé d'Oxygène Atomique et de son Interaction avec les Matériaux," Thesis, Spécialité Sciences des Matériaux, No. 207, Ecole Nationale Supérieure de l'Aéronautique et de l'Espace, Toulouse, France, Dec. 1996, pp. 1–186.

[19]Cross, J. B., Koontz, S. L., and Hunton, D. E., "Flight Mass-Spectrometer Calibration in a High-Velocity Atomic Oxygen Beam," *Journal of Spacecraft and Rockets*, Vol. 32, No. 3, 1995, pp. 496–501.

[20]Catherine, Y., "Croissance de Couches Minces sous Flux d'Ions," *Journées d'Études "Oléron 87" sur l'Interaction des Plasmas Froids-Matériaux*, Les Editions de Physique, Les Ullis, France, 1987, pp. 319–340.

[21]Clouet, P., Epaillard, F., and Segui, Y., "Plasmas Froids et Polymères," *Journées d'Études "Oléron 87" sur l'Interaction des Plasmas Froids-Matériaux*, Les Editions de Physique, Les Ullis, France, 1987, pp. 429–464.

[22]Van Eesbeek, M., Levadou, F., Tupikov, V. I., Cherniavsky, A. I., Khatipov, S. A., Milinchuk, V. K., and Stepanov, V. F., "Degradation of Teflon PTFE and FEP Exposed to Far UV Radiation," *Proceedings of the Sixth International Symposium on Materials in a Space Environment*, European Space Agency, Noordwijk, The Netherlands, 1994, pp. 149–164.

[23]Van Eesbeek, M., Levadou, F., Skurat, V. E., Dorofeev, Y. I., Vasilets, V. N., and Barbashev, E. A., "Degradation of FEP due to VUV and Atomic Oxygen Exposure," *Proceedings of the Sixth International Symposium on Materials in a Space Environment*, European Space Agency, Noordwijk, The Netherlands, 1994, pp. 165–173.

[24]Koontz, S. L., Leger, L. J., Albyn, K., and Cross, J. B., "Vacuum Ultraviolet Radiation/Atomic Oxygen Synergism in Materials Reactivity," *Journal of Spacecraft and Rockets*, Vol. 27, No. 3, 1990, pp. 346–348.

[25]Banks, B. A., and Rutledge, S. K., "Low Earth Orbital Atomic Oxygen Simulation for Materials Durability Evaluation," *Fourth International Symposium on Spacecraft Materials in a Space Environment*, CERT–ONERA, Toulouse, France, 1988, pp. 371–392.

[26]Vered, R., Lempert, G. D., Grossman, E., Haruvy, Y., Marom, G., Singer, G., and Lifshitz, Y., "Atomic Oxygen Erosion of Teflon FEP and Kapton H by Oxygen from Different Sources: Atomic Force Microscopy and Complementary Studies," *Proceedings of the Sixth International Symposium on Materials in Space Environment*, European Space Agency, Noordwijk, The Netherlands, 1994, pp. 175–181.

[27]Haris, I. L., Chambers, A. R., Roberts, G. T., and Van Eesbeek, M. B. J., "The Laboratory Testing of Silver and Polymeric Materials in Atomic Oxygen Flows," *Proceeedings of the Sixth International Symposium on Materials in a Space Environment*, European Space Agency, ESA-SP-368, Noordwijk, The Netherlands, 1994, pp. 195–200.

[28]Leger, L. J., Koontz, S. L., Visentine, J. T., and Cross, J. B., "Laboratory Investigations Involving High-Velocity Oxygen Atoms," *Fourth International Symposium on Spacecraft Materials in a Space Environment*, CERT–ONERA, Toulouse, France, 1988, pp. 393–404.

I. D. Boyd
Associate Editor

United States Postal Service

Statement of Ownership, Management, and Circulation

1. Publication Title	2. Publication Number	3. Filing Date
Journal of Spacecraft and Rockets	0 0 2 2 _ 4 6 5 0	12/1/98
4. Issue Frequency	5. Number of Issues Published Annually	6. Annual Subscription Price
Bi-monthly	6	$45/$75

7. Complete Mailing Address of Known Office of Publication *(Not printer) (Street, city, county, state, and ZIP+4)*: 1801 Alexander Bell Drive, Reston, VA, 20191 — Contact Person: Mary Ellen Lanham; Telephone: 703.264.7577

8. Complete Mailing Address of Headquarters or General Business Office of Publisher *(Not printer)*: AIAA American Institute of Aeronautics and Astronautics (above)

9. Full Names and Complete Mailing Addresses of Publisher, Editor, and Managing Editor *(Do not leave blank)*

Publisher *(Name and complete mailing address)*: Norma Brennan (AIAA-above)

Editor *(Name and complete mailing address)*: E.Vincent Zoby, NASA Langley Research Center, Hampton, VA

Managing Editor *(Name and complete mailing address)*: Mary Ellen Lanhar (AIAA-above)

10. Owner *(Do not leave blank. If the publication is owned by a corporation, give the name and address of the corporation immediately followed by the names and addresses of all stockholders owning or holding 1 percent or more of the total amount of stock. If not owned by a corporation, give the names and addresses of the individual owners. If owned by a partnership or other unincorporated firm, give its name and address as well as those of each individual owner. If the publication is published by a nonprofit organization, give its name and address.)*

Full Name	Complete Mailing Address
American Inst. of Aeronautics and Astronautics	1801 Alexander Bell Dr. Reston, VA, 20191

11. Known Bondholders, Mortgagees, and Other Security Holders Owning or Holding 1 Percent or More of Total Amount of Bonds, Mortgages, or Other Securities. If none, check box → ☐ None

Full Name	Complete Mailing Address

12. Tax Status *(For completion by nonprofit organizations authorized to mail at nonprofit rates) (Check one)*
The purpose, function, and nonprofit status of this organization and the exempt status for federal income tax purposes:
☐ Has Not Changed During Preceding 12 Months
☐ Has Changed During Preceding 12 Months *(Publisher must submit explanation of change with this statement)*

PS Form **3526**, September 1998 *(See Instructions on Reverse)*

13. Publication Title: Journal of Spacecraft and Rockets			14. Issue Date for Circulation Data Below: November/December 1998
15. Extent and Nature of Circulation			Average No. Copies Each Issue During Preceding 12 Months	No. Copies of Single Issue Published Nearest to Filing Date
a. Total Number of Copies *(Net press run)*			2350	2500
b. Paid and/or Requested Circulation	(1)	Paid/Requested Outside-County Mail Subscriptions Stated on Form 3541. *(Includes advertiser's proof and exchange copies)*	1826	1977
	(2)	Paid In-County Subscriptions *(Include advertiser's proof and exchange copies)*		
	(3)	Sales Through Dealers and Carriers, Street Vendors, Counter Sales, and Other Non-USPS Paid Distribution		
	(4)	Other Classes Mailed Through the USPS		
c. Total Paid and/or Requested Circulation *(Sum of 15b. (1), (2),(3),and (4))*			1826	1977
d. Free Distribution by Mail *(Samples, complimentary, and other free)*	(1)	Outside-County as Stated on Form 3541	50	50
	(2)	In-County as Stated on Form 3541		
	(3)	Other Classes Mailed Through the USPS		
e. Free Distribution Outside the Mail *(Carriers or other means)*				
f. Total Free Distribution *(Sum of 15d. and 15e.)*			50	50
g. Total Distribution *(Sum of 15c. and 15f)*			1876	2027
h. Copies not Distributed			474	473
i. Total *(Sum of 15g. and h.)*			2350	2500
j. Percent Paid and/or Requested Circulation *(15c. divided by 15g. times 100)*			78%	79%

16. Publication of Statement of Ownership
☐ Publication required. Will be printed in the _____ issue of this publication. ☐ Publication not required

17. Signature and Title of Editor, Publisher, Business Manager, or Owner: Norma Brennan, Publications Director — Date: 12/1/98

I certify that all information furnished on this form is true and complete. I understand that anyone who furnishes false or misleading information on this form or who omits material or information requested on the form may be subject to criminal sanctions (including fines and imprisonment) and/or civil sanctions (including civil penalties).

Instructions to Publishers

1. Complete and file one copy of this form with your postmaster annually on or before October 1. Keep a copy of the completed form for your records.
2. In cases where the stockholder or security holder is a trustee, include in items 10 and 11 the name of the person or corporation for whom the trustee is acting. Also include the names and addresses of individuals who are stockholders who own or hold 1 percent or more of the total amount of bonds, mortgages, or other securities of the publishing corporation. In item 11, if none, check the box. Use blank sheets if more space is required.
3. Be sure to furnish all circulation information called for in item 15. Free circulation must be shown in items 15d, e, and f.
4. Item 15h., Copies not Distributed, must include (1) newsstand copies originally stated on Form 3541, and returned to the publisher, (2) estimated returns from news agents, and (3), copies for office use, leftovers, spoiled, and all other copies not distributed.
5. If the publication had Periodicals authorization as a general or requester publication, this Statement of Ownership, Management, and Circulation must be published; it must be printed in any issue in October or, if the publication is not published during October, the first issue printed after October.
6. In item 16, indicate the date of the issue in which this Statement of Ownership will be published.
7. Item 17 must be signed.

Failure to file or publish a statement of ownership may lead to suspension of Periodicals authorization.

PS Form **3526**, September 1998 *(Reverse)*